

# Reducing numerical work in non-linear parameter identification

Emoke Imre<sup>1\*</sup>, Peter Berzi<sup>2</sup>, Csaba Hegedus<sup>3</sup>, Sándor Kovacs<sup>3</sup>, Levente Kovacs<sup>2</sup>

<sup>1</sup> HBM Systems research center, Obuda University, Hungary

<sup>2</sup> AIAM Doctoral School, Obuda University, Hungary

<sup>3</sup> Department of Numerical Analysis, Eotvos Lorand University, Budapest, Hungary

\* Corresponding author, e-mail: [imreemok@gmail.com](mailto:imreemok@gmail.com)

## Abstract

The real-life merit functions have an unimaginable complexity of an  $M$ -dimensional topography, where  $M$  is the number of the parameters. It is shown that there is an underlying noise-free merit function, called follower merit function which can be constructed from simulated, noise-free data using the solution of a Least Squares minimization. The difference of the real-life merit and follower merit function is controlled by the norm of the noise-free error vector. Therefore, the non-important local minima arisen from the noise can be skipped during such minimization that apply adjustable, large step sizes, depending on the norm of the noise-free error vector.

The non-linear minimization can be difficult even in the case of some strictly convex, non-negative merit functions if the geometry is highly asymmetric or if the global minimum is quasi-degenerated. The suggested hierarchical minimisation - based on the implicit function of a projection map - makes the minimisation in two steps. In the first step some parameters are eliminated with conditional minimisation, resulting in a kind of deepest section of the merit function, called clever section with respect to the remainder parameters. Then the clever section is minimized. The method can be used to handle a quasi-degenerate global minimum, in sensitivity analyses, reliability testing.

## Keywords

non-linear minimization, implicit function theorem, sub-minimization, inverse problem, parameter identification, least-squares merit function

## 1 Introduction

### 1.1 Definitions

Let us assume that the model is given by a function  $u : R^+ \times R^M \rightarrow R$ ;  $(t, \mathbf{p}) \rightarrow u(t, \mathbf{p})$ ; where  $R^+ \ni t$  is the time variable,  $D \ni \mathbf{p}$  is the parameter vector with  $M$  elements; the  $D$  is the simply connected and compact parameter domain contained by  $R^M$ . We can introduce a partial function  $v_p(t) = u(t, \mathbf{p})$  and define its graph  $G : R^M \rightarrow R^2$  as  $F = G(\mathbf{p}) = \{R^2 \ni (t, v_p(t))\}$ .

In the direct problem - for a fixed value of  $\mathbf{p}$  - the graph of the partial function  $v_p(t) = u(t, \mathbf{p})$ , expressed as  $F = G(\mathbf{p})$ , is determined. In the inverse problem the goal is the determination of the parameter vector  $\mathbf{p}$  for a given graph  $F$ , expressed as  $\mathbf{p} = G^{-1}(F)$ .

In the discrete formulation, instead of the graph, only some points of the graph of the partial function  $v_p(t)$  are considered, denoted by  $v_p(t^i)$ . These values are compiled into a so-called data vector  $\mathbf{f}$ . The function  $\mathbf{u}(\mathbf{p}) : R^M \rightarrow R^N$ ,  $(\mathbf{p}) \rightarrow \mathbf{u}(\mathbf{p})$ , called model response function, containing  $N$  elements, can be constructed from the copies of  $u(t, \mathbf{p})$  in such a way that times  $t_1 \dots t_N$  - the elements of the so-called sampling time vector  $\mathbf{t}$  - are substituted for the time variable  $t$  in  $u(t, \mathbf{p})$ .

The solution of the direct problem is the value of the model response function  $\mathbf{f} = \mathbf{u}(\mathbf{p})$  for a given  $\mathbf{p}$  which is called a simulated data vector.

In the inverse problem, for a fixed value of  $\mathbf{f}$  and  $\mathbf{t}$ , the goal is the determination of the parameter vector  $\mathbf{p}$ , from the equation  $\mathbf{h}(\mathbf{p}) = \mathbf{f} - \mathbf{u}(\mathbf{p}) = 0$ , expressed as  $\mathbf{p} = \mathbf{u}^{-1}(\mathbf{f})$ .

The solution of a non-linear system of equations  $\mathbf{f} - \mathbf{u}(\mathbf{p}) = 0$  is needed, which generally has weak solution only, since generally  $N > M$ . The weak solution is the global minimizing vector  $\mathbf{p}_{\min}$  of the least squares objective function called real-life merit function which is the norm squares of the error vector  $\mathbf{h}(t, \mathbf{p}) = u_m(t_i) - u(t, \mathbf{p})$ :

$$F(\mathbf{p}) = \sum_{i=1}^N [u_m(t_i) - u(t_i, \mathbf{p})]^2 \quad (1)$$

where  $t_i$  are the sampling times ( $i=1,2,..N$ ),  $m$  indicates the measured value and  $p$  is the parameter vector containing  $M$  parameters which may influence (partly linearly and partly non-linearly) the solution  $u(t, p)$  of the model. The minimum is to zero for a simulated data vector, but is not zero if the data vector is noisy, due to measurement errors, numerical inaccuracies and modeling errors.

## 1.2 Difficulties in non-linear parameter identification

### 1.2.1 Problems in non-linear minimisation

The solution of a *linear* inverse problem can be determined without iteration, eg., by the SVD algorithm, which helps in the ill-posed cases as well. However, the multidimensional, non-linear minimization generally needs iterations and it is generally difficult if the model has several unknown parameters since (i) too many local minima of the real-life merit function may occur due to the noise, moreover, (ii) the geometry of the valley of the global minimum could be asymmetric and (iii) the minimum can be quasi-degenerated.

The first problem - the unimaginable complexity of an  $N$ -dimensional topography [1] - is treated in the literature by some ways. A trial and error process is used in every case, when not significant decrease in the error is attained, the process may restart from a new starting vector.

The methods, which include one-dimensional minimisation iteration steps, are generally coupled with some new starting vector determination methods (eg., the simulated annealing method, which steps away from a local minimum using probability theory methods, see eg. [1] or by fitting a smooths hypersurface locally [2]).

The non-linear minimization methods without one-dimensional minimisation (eg., simplex method [1], or secant method see Section 6) are considered as effective tool in case of a few parameters [1], the reason of the better performance is related to the fact that these may skip some critical points, as shown here.

The quasi-degenaret minimum problem is treated generally by regularization ([3]), the asymmetric shape of the vally is an unsolved problem.

### 1.2.2. Problems in reliability testing

The singularity of the Hesse matrix at a minimum  $\mathbf{p}_{\min}$  gives information on local uniqueness. If the global minimum is degenerated, infinite many solutions may exists, some parametererts are dependent. In case of linear inverse problems, the global uniqueness is met in case of local non-singularity.

The solution of a real-life inverse problem  $\mathbf{p}_{\min}$  is approximate with some error. Using the linear model, the computation of the standard deviation of the parameters is possible, assuming normally distributed noise (residuals) [1]. The geometrical interpretation is related to the orthogonal projection of a confidence domain, which is defined by a level line of a kind of noise-free merit function (Fig. 1), with symmetry related to the individual parameters. The unsolved problem is the parameter error in case of non-normal noise.

In case of non-linear inverse problems, the global uniqueness is not met in case of local non-singularity. The computation of the standard deviation is possible, similarly to the linear case, assuming normally distributed noise [1]. It has similar geometrical meaning: it is the orthogonal projection of the confidence domain, related to a noise-free, linearized merit function. Some unsolved, additional questions are the global uniqueness, and the parameter error in case of non-normal noise and the non-symmetry with respect to the individual parameters.

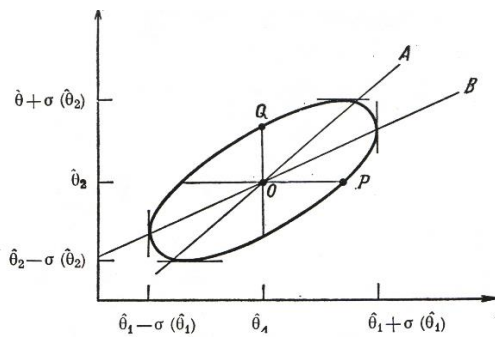


Fig. 1 Confidence domain of 68.3%, the standard deviation in case of normally distributed noise (after [1]).

### 1.3 The content of paper

To overcome the foregoing difficulties, three new concepts are presented and discussed. The first concept is the Hierarchical minimisation which means the split of Hierarchical minimisation into two parts with lower dimensions, such that different minimisation methods may be used in each part.

The hierarchical inverse problem concept is mathematically explained by the implicit function theorem. The related map is the orthogonal projection of the graph of the merit function onto a plane  $\langle F, \mathbf{x} \rangle$ , and the implicit function  $y = \mathbf{g}(\mathbf{x})$  is related to the fold of the image of the map.

The second concept is related to the use of the section of the merit function along the fold, defined in the HIP concept. The so called clever section can be used to estimate the global minimum without minimization if some independent information for the  $\mathbf{x}_{\min}$  part of the global minimum is available. In this case  $\mathbf{y}_{\min} = \mathbf{g}(\mathbf{x}_{\min})$ . The one-dimensional clever section - depending on a single parameter - is a deepest sensitivity section which can be used for sensitivity analyses and reliability testing.

The third concept is the follower, noise-free merit function - the best possible noiseless approximation of the real-life merit function - which can equally be used for minimisation and reliability testing. The real-life merit function has too many local minima with nearly the same merit function value around the global minimiser  $\mathbf{p}_{\min}$ . The global uniqueness of the solution can be interpreted by the follower here. The obstruction domain for minimisation is a parameter error domain, defined by a level line of the follower merit function here.

The follower is not known a priori but can be determined afterwards using the global minimiser  $\mathbf{p}_{\min}$ . It is shown that the difference of the two functions is dependent on the actual size of the noise-free residuals. Due to the similarity, the decreasing direction of the follower can be estimated during minimisation by the noisy (real-life) merit function on a part of the parameter domain - aiding minimisation - if the step size is large enough, eg. dependent on the actual size of the noise-free residuals.

In the paper two examples are presented. The step size of the secant method, a non-linear minimization methods, without one-dimensional minimisation ([6 to 8]) is analysed. It is shown that this method is theoretically able to skip some local minima since its step size is dependent on the actual size of the noise-polluted residuals. The example also illustrates how the linearly dependent parameters can be eliminated as an application of the Hierarchical minimisation concept.

The second example shows that such non-iterative (automatic) global minimisation related to the injective solutions of linear PDE-s can be given that gives reliability information as well. The model solution was expressed with 8 parameters, 4 non-linearly dependent parameters. Variants were given where the number of the latter was decreased to 1 by using information concerning the analytical properties of the model and some approximations. The numerical work depended on the number of non-linearly dependent parameters exponentially and was much less than the solution found with the conjugate gradient method coupled with a new starting vector determination method for a decreased nonlinearly dependent parameter numbers.

### 3 Hierarchical minimisation or inverse problem solution

#### 3.1 General

##### 3.1.1. Definition

The parameter space can be split into the direct sum of two subspaces:

$$\mathbf{p} = [\mathbf{p}_1, \mathbf{p}_2], \quad \mathbf{p}_1 \in D_1 \subset \mathbb{R}^J, \mathbf{p}_2 \in D_2 \subset \mathbb{R}^{M-J} \quad (2)$$

The first inverse problem is a conditional minimization:

$$F(\mathbf{p}_1, \mathbf{p}_2) = \min_{\mathbf{p}_2}, \quad \mathbf{p}_1 = \text{const}, \forall \mathbf{p}_2 \in D_2 \subset \mathbb{R}^{M-J} \quad (3)$$

the solution of which is the relation  $\mathbf{p}_1 = \mathbf{a}(\mathbf{p}_2)$ . If this is inserted then an  $M-J$  dimensional minimal section of  $\mathbf{p}_2$  the section of the original merit function, denoted by  $F[\mathbf{a}(\mathbf{p}_2), (\mathbf{p}_2)]$  is resulted which depends only on  $\mathbf{p}_2$ .

The second inverse problem:

$$F[\mathbf{a}(\mathbf{p}_2), \mathbf{p}_2] = \min_{\mathbf{p}_2}, \quad \mathbf{p}_2 \in D_2 \subset \mathbb{R}^{M-J} \quad (4)$$

is the minimization of  $F[\mathbf{a}(\mathbf{p}_2), (\mathbf{p}_2)]$ .

##### 3.1.2 Definition

The section  $F[\mathbf{a}(\mathbf{p}_2), (\mathbf{p}_2)]$  is called minimal or clever section of  $\mathbf{p}_2$ .

##### 3.1.3 Statement

The solution of the hierarchical minimisation is trivially equivalent to the original one if the Hessian of  $F$  with respect to  $\mathbf{p}_1$  is globally positive definite, which is met e.g., if the function  $F$  is strictly convex.

#### 3.2 Mathematical explanation

We change the notation so that subscripts can be omitted in the index. We use  $\mathbf{y}$  i  $\mathbf{x}$  instead of  $\mathbf{p}_1$  and  $\mathbf{p}_2$ .

##### 3.2.1 The definition of the projection map

Let us consider a strictly convex, non-negative, analytic (Least Squares merit) function  $F(\mathbf{p}) : D \subset \mathbb{R}^{n+m} \rightarrow \mathbb{R}^1$  with simply connected, compact domain  $D$  and with the arbitrary  $\mathbf{p}=(\mathbf{x}, \mathbf{y})$  arbitrary direct sum decomposition of  $D$ ,  $n+m=l$ . The global minimum is  $(\mathbf{a}, \mathbf{b})$ , where  $F$  has the only critical point.

Let us consider the orthogonal projection of the graph of  $F$  onto the  $F$ - $\mathbf{x}$  coordinate plan in the total Euclidean space generated by the graph, described by  $F(\mathbf{x}, \mathbf{y})$ . The projection planes are  $\mathbf{x}=\text{const}$  coordinate planes, the critical values of the map - where the fold of the projection is found - are related to the  $F_y(\mathbf{x}, \mathbf{y})=f(\mathbf{x}, \mathbf{y})=0$ .

##### 3.2.2 The implicit function theorem in case of the a prejection of the graph a strictly convex function

The implicit function theorem [4, 5] is applied in the case of the projection of the graph of a strictly convex, non-negative, analytic (Least Squares merit) function to describe the fold where the condition is met  $F_y(\mathbf{x}, \mathbf{y})=f(\mathbf{x}, \mathbf{y})=0$  as follows. Starting from a direct product decomposition, the goal is to construct a function  $g: \mathbb{R}^n \rightarrow \mathbb{R}^m$  whose graph  $(\mathbf{x}, g(\mathbf{x}))$  is precisely the set of all  $(\mathbf{x}, \mathbf{y})$  such that the  $F_y(\mathbf{x}, \mathbf{y})=f(\mathbf{x}, \mathbf{y})=0$ .

Let us consider the critical point at the global minimum  $(\mathbf{a}, \mathbf{b}) = (a_1, \dots, a_n, b_1, \dots, b_m)$  where  $F_y(\mathbf{x}, \mathbf{y}) = \mathbf{f}(\mathbf{x}, \mathbf{y}) = \mathbf{0}$ , the zero is element of  $\mathbf{R}^m$ . If the matrix  $F_y(\mathbf{x}, \mathbf{y}) = [(\partial f_i / \partial y_j)(\mathbf{a}, \mathbf{b})]$  has full rank, then there exists an open set  $U$  containing  $\mathbf{a}$ , an open set  $V$  containing  $\mathbf{b}$ , and a unique, analytic, injective function  $\mathbf{g}: U \rightarrow V$  such that

$$\{\mathbf{x}, \mathbf{g}(\mathbf{x}) | \mathbf{x} \in U\} = \{\mathbf{x}, \mathbf{y} | \mathbf{x} \in U, \mathbf{f}(\mathbf{x}, \mathbf{y}) = \mathbf{0}\} \quad (5)$$

It follows from the injectivity, that if parameter vector  $\mathbf{x}_{\min}$  is the part global minimum, then  $\mathbf{y}_{\min} = \mathbf{g}(\mathbf{x}_{\min})$ .

### 3.2.3 Consequences

Consequences of the strict convexity are as follows.

1. The implicit function points are the single conditional minima of  $F$  since  $F_y(\mathbf{x}, \mathbf{y}) = [(\partial f_i / \partial y_j)(\mathbf{a}, \mathbf{b})]$  is globally positive definite.
2. The implicit function is globally unique following from the strict convexity.
3. The clever sections (and, graphs of implicit functions) related to various  $\mathbf{x} < \mathbf{x} < \mathbf{p}$  have the same lattice structure like the lattice structure of subspaces of the  $R^M$  generated by the parameter space at the direct product decomposition. If the split of the parameter space is such that  $\mathbf{x} < \mathbf{x}$  then the clever section  $F[\mathbf{g}(\mathbf{x}), \mathbf{x}]$  contains  $F[\mathbf{g}(\mathbf{x}), \mathbf{x}]$  where  $\mathbf{x} < \mathbf{x}$ . The  $F[\mathbf{g}(\mathbf{x}), \mathbf{x}]$  can equally be defined using  $F[\mathbf{g}(\mathbf{x}), \mathbf{x}]$  or  $F(\mathbf{p})$ .

## 4 Follower merit function

### 4.1 General

#### 4.1.1 The definition of the follower merit function

The so-called follower merit function  $F(\mathbf{p})$  is defined as the norm squares of the simulated error vector, computed by using the simulated, noise-free data, generated with  $\mathbf{p}_{\min}$ :

$$F(\mathbf{p}) = \sum_{i=1}^N h_i(\mathbf{p})^2 = \sum_{i=1}^N [u(t_i, \mathbf{p}) - u(t_i, \mathbf{p}_{\min})]^2 \quad (6)$$

where  $u(t_i, \mathbf{p}_{\min})$ , the simulated, noise-free data and  $u(t, \mathbf{p})$  is the model solution,  $t_i$  ( $i=1..N$ ) are sampling times.

#### 4.1.2 The definition of the noise

The noise  $z_i$  can be expressed from the following decomposition, after the determination of the global minimum of the merit function and the simulated data:

$$u_m(t_i) = u(t_i, \mathbf{p}_{\min}) + z_i \quad (7)$$

where  $\mathbf{p}_{\min}$  minimiser,  $u(t, \mathbf{p})$  is the model solution.

#### 4.1.3 The definition of the similarity domain and the parameter error domain

The parameter space is split into two parts with the level surface of the noise-free merit function related to the :global minimum of the real-life merit function. The distribution-free parameter error domain, similarly to the statistical error domain (Fig. 1) is defined as the following sublevel set of the follower merit function:

$$E = \{\mathbf{p} \in D | F(\mathbf{p}) \leq c = F(\mathbf{p}_{\min})\} \quad (8)$$

where the real-life merit function contains several local minima with about the same value. The complement domain - far from the global minimum where

$$\|h'(\mathbf{p})\|^2 > \|z\|^2 \quad (9)$$

is met - is defined as similarity domain. In here the follower can be approximated by the real-life merit function.

## 4.2 The relation of the two merit functions

### Statement

Using the foregoing, the two merit functions: the follower merit function  $F$  and the real-life merit function  $F$  has the following relationship:

$$F(\mathbf{p}) = \sum_{i=1}^N [h_i(\mathbf{p}) - z_i]^2 = F'(\mathbf{p}) - \sum_{i=1}^N [2h_i(\mathbf{p})z_i] + F(\mathbf{p}_{min}) \quad (10)$$

By using the Cauchy-Schwartz-Bunyakovskij inequality:

$$\begin{aligned} F'(\mathbf{p}) - 2\|h'(\mathbf{p})\| \|z\| + F(\mathbf{p}_{min}) &= \|h'(\mathbf{p})\|^2 - 2\|h'(\mathbf{p})\| \|z\| + \|z\|^2 \\ \leq F(\mathbf{p}) &\leq \|h'(\mathbf{p})\|^2 + 2\|h'(\mathbf{p})\| \|z\| + \|z\|^2 = \\ F'(\mathbf{p}) + 2\|h'(\mathbf{p})\| \|z\| + F(\mathbf{p}_{min}) \end{aligned} \quad (11)$$

The difference of the two functions can be expressed as follows:

$$-2\|h'(\mathbf{p})\| \|z\| + \|z\|^2 \leq F(\mathbf{p}) - F'(\mathbf{p}) \leq 2\|h'(\mathbf{p})\| \|z\| + \|z\|^2 \quad (12)$$

According to Eq (12), the difference of the two function seems to be small for fixed, small noise, being controlled however by the norm of the noise-free error vector (which is a pseudo-metric expressing a distance from the global minimum where it is zero, see section 5.2.1).

## 5. Practical use of concepts and methods

### 5.1 Use of split minimisation

#### 5.1.1 Elimination of the linearly dependent parameters

##### Definition

If the model solution can be written as the scalar product  $u(t, \mathbf{p}) = \mathbf{y} \cdot \mathbf{b}(t, \mathbf{x})$ , then the elements of  $\mathbf{y}$  are linearly dependent parameters.

##### Statement

In case of  $\mathbf{y}$  linearly dependent parameters, the Hessian matrix  $[(\partial f_i / \partial y_j)(\mathbf{a}, \mathbf{b})]$  has the following form:

$$\begin{aligned} &\langle \mathbf{a}, \mathbf{a} \rangle && \langle \mathbf{a}, \mathbf{b} \rangle && \langle \mathbf{a}, \mathbf{w} \rangle \\ &\langle \mathbf{b}, \mathbf{a} \rangle && \langle \mathbf{b}, \mathbf{b} \rangle && \langle \mathbf{b}, \mathbf{w} \rangle \\ &&&&& \langle \mathbf{w}, \mathbf{w} \rangle \end{aligned} \quad (13)$$

This is a Gram matrix. If the vectors are linearly independent, which is met if the partial derivatives of the merit function with respect to the elements of  $\mathbf{y}$  are linearly independent, then it is positive definite. It follows that if  $\mathbf{y}$  linearly dependent then it can be eliminated by linear subminimisation.

### Consequence

The most important practical application of the split minimisation is the elimination of the linear part of parameter vector through sub-minimisation. The linear subminimisation - a generalized linear inverse problem [1] - can be solved without iteration, eg., by the SVD or singular value decomposition (SVD) algorithm. The linearly dependent parameters can be eliminated by sub-minimisation before each function value evaluation in case of any non-linear minimization method.

#### 5.1.2 Use of the clever sections

Some kind of regularization method is possible to be used as follows. The clever section and the related implicit function  $\mathbf{g}(\mathbf{x})$  can be used to estimate the global minimum of  $F[\mathbf{x}, \mathbf{g}(\mathbf{x})]$  without minimization in case the parameter vector value  $\mathbf{x}_{\min}$  of the global minimum is available. In this case  $\mathbf{y}_{\min} = \mathbf{g}(\mathbf{x}_{\min})$ . This follows from the fact that the implicit function is analytic, simple curve.

The one-dimensional clever sections of the follower and the real-life merit functions can simultaneously be represented in the 2-dimensional plane and can be used for uniqueness testing and parameter error estimation. The generalized standard deviation (Fig. 2) can be defined as the size of the error domain in plus or minus directions. Being the error domain non-symmetric, the orthogonal projection of its diameter onto parameter axis  $p^i$  is reasonable to be used.

## 5.2 Minimisation with the follower

### 5.2.1 General

Definition of pseudo-metrics

The definition of a metric on the set  $\{\alpha, \beta, \gamma, \dots\}$  is as follows:

$$1) \quad d(\alpha, \beta) \geq 0, \quad 2) \quad d(\alpha, \beta) = 0 \Leftrightarrow \alpha = \beta, \quad 3) \quad d(\alpha, \beta) = d(\beta, \alpha), \quad 4) \quad d(\alpha, \gamma) \leq d(\alpha, \beta) + d(\beta, \gamma) \quad (14)$$

If the second is not met, a pseudometric is defined. Two pseudo-metrics can be introduced:

$$d_F(\mathbf{a}, \mathbf{b}) = |F(\mathbf{a}) - F(\mathbf{b})| \quad (15)$$

using the merit function  $F$  or  $F$  where  $D \ni \mathbf{a}, \mathbf{b}$  are parameter vectors with  $M$  elements .

### Statement

According to Eq (12), the difference between the follower and the real-life merit functions is bounded by a term which is linearly related to the norm of the noise-free, follower at a fixed noise vector. If the norm of the fixed noise vector is relatively small, not larger than the norm of the noise-free error vector (this conditions are met on the similarity domain), then theoretically (i) the follower merit function values can be approximated by real-life merit function values, decreasing directions can be assessed, (ii) the noise-free error vector and the noisy error vectors have the same order of magnitude, both indicate the distance from the global minimum, being pseudo-metrics.

### 5.2.2 Suggested methods

#### Step size control

In the minimization methods not using line minimization, the step size generally can theoretically be selected to be large enough to skip the critical points due to the noise (e.g. if the sign of the difference of the merit function for  $F$  and  $F$  at any two points is identical).

#### Global coordinate grid in case of convex follower

In the case of strictly convex follower, decreasing convex level surfaces (and a minimum) can trivially be bracketed by tangent coordinate hyperplanes generated from coordinate grid points, using real-life merit function values. As a result, the non-linear inverse problems can be solved without iteration, with function value evaluations in a coordinate grid. A global coordinate grid can be used - with a projection algorithm - to determine the one-dimensional clever sections. The real-life merit functions values are computed in the points of a coordinate grid in a nested cycle. The one-dimensional clever section point of each parameter  $x_i$  can be determined by projections along each respective coordinate planes  $x^{i,j} = \text{const.}$  such that for a given parameter value  $x^{i,j}$  all grid values are considered and, the parameter values related to the conditional minimum is selected (Fig. 3).

The grid dimension is determined by the number of the non-linearly dependent parameters, since if each function value evaluation is preceded by a linear subminimisation, the linearly dependent parameters are eliminated. (It may occur that only one non-linearly dependent parameter remains.) In this way the values of the clever section of parameter vector part  $\mathbf{x}$  is determined in the given mesh point denoted by  $F[g(\mathbf{x}), \mathbf{x}]$ , which can be used in case of quasi-degenerated global minimum (instead of bracketing).

In the case of strictly convex follower, once the minimum of the real-life merit function is determined, the same algorithm can be reused to determine the one-dimensional clever sections of the follower merit functions, too. The difference them at the global minimum can be used to determine the error domain (Fig. 2) and, to observe the difference of the follower and real-life merit functions in the similarity domain. The distance of the grid values can be selected as the diameter of the error domain, determined beforehand using simulated noise-free and noise-polluted data (see the Appendix).

*Local coordinate grid*

A local coordinate grid generated in the subspace of some important parameters can be used to find a decreasing direction and a new starting vector in this direction. The grid search is effective on condition that the sign of the difference of the merit function values at the grid points is identical, which can be attained if the point distance is controlled by the merit function value and the sensitivity of the parameters. The distance is advisable to be smaller than the diameter of the geometrical parameter error domain, at least close to the global minimum.

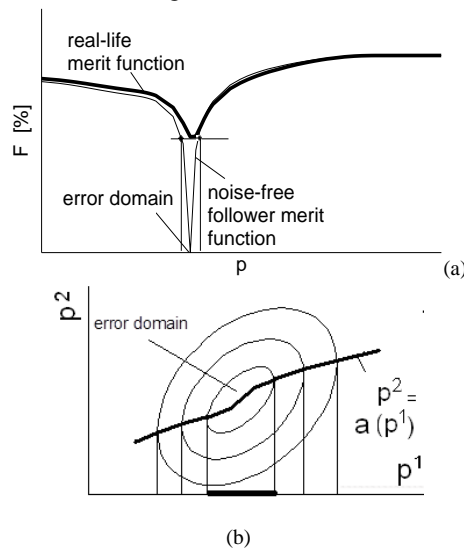


**Fig. 2.** The one dimensional clever section of merit functions and the parameter error domain (a) in the total space (b) in the parameter space. Being the error domain non-symmetric, the orthogonal projection of its diameter onto parameter axis  $p^i$  is reasonable to be used. See its value in App.

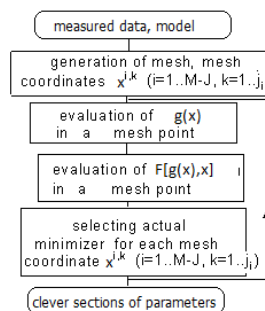


**Fig. 3.** The determination of the approximate one-dimensional clever sections by elimination, projection and minimum search in a nested cycle system. A coordinate mesh is generated in the M-J dimensional space of the nonlinearly dependent parameters, J linearly dependent parameters are eliminated.

**6 Example 1 - secant method**

In the secant-type methods the step size is controlled by the real-life merit function  $F$  value (i.e., norm square of the noise-polluted error vector), and a similar variable basically controls the difference of the two functions, also. These method iare shortly presented as follows.

6.1 Wolfe method

In the secant method [6,7]  $n+1$  trial solutions for the parameter vector and the related residual or error vector  $(\mathbf{p}_i, \mathbf{h}(\mathbf{p}_i))$  ( $i = 0, \dots, n$ ) are used to compute a new parameter vector:

$$\begin{bmatrix} \mathbf{p} \\ \mathbf{h}(\mathbf{p}) \end{bmatrix} \approx \begin{bmatrix} \mathbf{p}_0 \\ \mathbf{h}(\mathbf{p}_0) \end{bmatrix} + \begin{bmatrix} \mathbf{A}_p \\ \mathbf{A}_r \end{bmatrix} \mathbf{q} \tag{16}$$

where  $m$  is the number of sampling times,  $n$  is parameter number.  $\mathbf{A}_p = [\mathbf{p}_0 - \mathbf{p}_1, \dots, \mathbf{p}_0 - \mathbf{p}_n]$ ,  $\mathbf{A}_r = [\mathbf{h}(\mathbf{p}_0) - \mathbf{h}(\mathbf{p}_1), \dots, \mathbf{h}(\mathbf{p}_0) - \mathbf{h}(\mathbf{p}_n)]$  and  $\mathbf{q}^T = [q^1, \dots, q^n]$  is a vector with  $n$  coefficients of secant method, called as an auxiliary variable.

The  $q$  in the one-dimensional case is equal to  $h(p_1) / [h(p_0) - h(p_1)]$ , similar formula is valid in multidimensional case. The absolute value of the multiplier  $h(p_1)$  is a pseudometric, expressing a distance from the global minimum. The step size is comparable with the controlling term of difference between the follower and the real-life merit function (see Eq (10)). Far from the global minimum, a large step from  $\mathbf{p}_0$  is resulted, allowing the skipping of some critical points. In other words, the in the secant method, the step size (related to the  $q$  coefficient) depends on the same variable as the difference between the follower and the real-life merit functions. These norms or merit function values are pseudometrics, being large far from the minimum and vice versa.

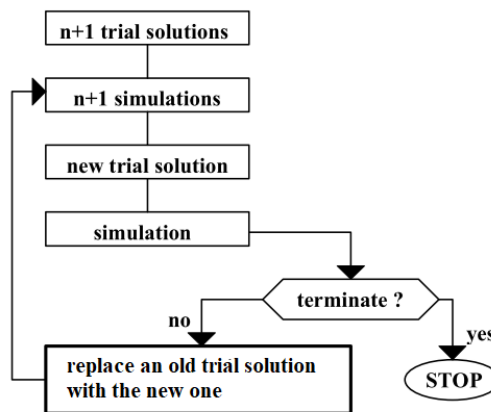
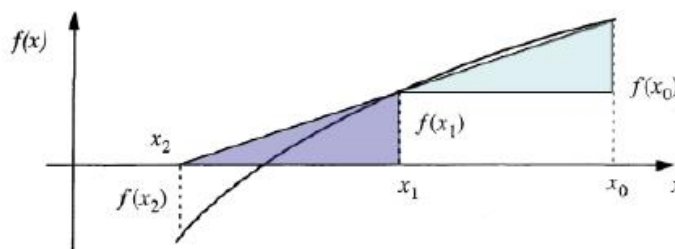
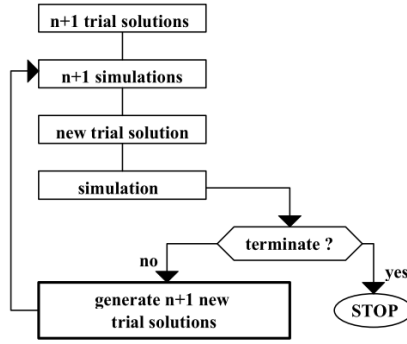
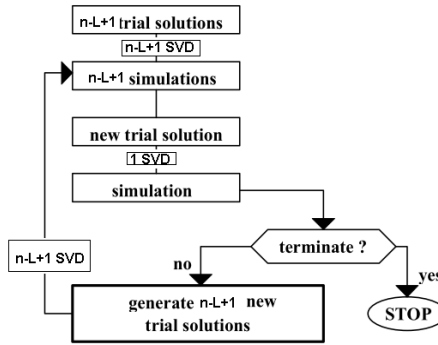


Fig. 4. (a) Secant method in 1D. Note that if the function value at  $x_1$  is the larger, then the step is the greater. (b) Flow diagram of Wolfe-secant method

a)



(b)



(c)

**Fig. 5.** Flow diagrams (a) Modified secant method (b) Modified shark secant method with linear subminimisation (each function value evaluation is preceded by a linear sub-minimisation).

### 6.2 The modified Wolfe method

Wolfe ([5]) suggested to select  $n+1$  new trial solutions for the next iteration by dropping the trial solution for which the norm of the error vector is the largest. This procedure fails when the norm of the new residual vector is the largest one. In the amended method ([2], Fig. 4), after determining  $\mathbf{p}_{n+1}$ , a second trial solution  $\mathbf{p}_{n+2}$  is determined. With matrix equation:

$$\begin{bmatrix} \mathbf{T}_p & \mathbf{0} \\ \mathbf{0} & \mathbf{T}_r \end{bmatrix} \begin{bmatrix} \mathbf{A}_p \\ \mathbf{A}_r \end{bmatrix} \mathbf{q}_2 = \begin{bmatrix} \mathbf{p}_0 - \mathbf{p}_{n+1} \\ \mathbf{h}(\mathbf{p}_0) \end{bmatrix} \quad (17)$$

where  $\mathbf{T}_p$  and  $\mathbf{T}_r$  are transformation diagonal matrices with elements:

$$t_p^i = \frac{p_{n+1}^i - p_{n+2}^i}{p_0^i - p_{n+1}^i}, t_r^i = h^i(\mathbf{p}_{n+1}) / h^i(\mathbf{p}_0) \quad (18)$$

The distance of  $\mathbf{p}_{n+1}$  and  $\mathbf{p}_{n+2}$  is related to the decrease of the error and the merit function between  $\mathbf{p}_{n+1}$  and  $\mathbf{p}_0$ . The  $n+1$  new trial solutions are selected from the new vectors as:

$$\mathbf{p}^i = \mathbf{p}_{n+1} + \mathbf{e}_i (\mathbf{p}_{n+2}^i - \mathbf{p}_{n+1}^i) \quad (19)$$

where  $\mathbf{e}^i$  is the  $i$ -th unit vector. The system of linear equations in the second rows of the matrix equations are solved by singular value decomposition (SVD).

The new auxiliary variable  $q_3$ , is determined from the first line of the matrix equation (17). In the one-dimensional case, it is a multiple of  $q$ , being equal to  $h(p_1)/h(p_2)*q$  [8]. A similar generalization is valid in the multidimensional case, described in [8]. It can be noted that the absolute value of the multiplier is a pseudometric again, expressing a distance from the global minimum, and the norm of this term is found in Equation (12). Far from the global minimum, it is large, a large step from  $p_1$  is determined (software is available [17]).

### 6.3 Elimination of the linearly dependent parameters

The most important practical application of the HIP in minimisation is the elimination of the linear part of parameter vector through sub-minimisation. The linear subminimisation can be solved by singular value decomposition (SVD) which can be added to any algorithm. If the linear part of the parameter vector is eliminated in The modified secant method (Fig. 5) then the numerical work is smaller since the number of the parameters is  $n-L$  instead of  $n$  where  $L$  is the number of the linearly dependent parameters. The size of matrices  $A_p$  and  $A_1$  is smaller. However, before each function value evaluation a linear sub-minimization using the SVD algorithm is needed.

**Table 1** Types of one dimensional oedometric dissipation tests with constant boundary condition

(Multistage) relaxation test	(MRT)
(Multistage) compression test	(MCT)

**Table 2** Types dissipation tests made with static penetrometers, modelled with cylindrical and spherical (ellipsoid) shaped domain.

Measured variable	dissipation test made by
Pore water pressure dissipation test, sensor on the shaft and/or on the tip	CPTu (static cone penetrometer)
Total stress dissipation test, sensor on the shaft and/or on the tip	CPT- piezo-lateral stress cell, CPT- DMT tip, CPT - CPT- $q_c$
Effective stress dissipation test, sensor on the shaft	CPT- $f_s$

**Table 3** Point-symmetric consolidation models [12]

$V$ or $\varepsilon$ boundary condition	1D (Oedometric models)	2D (Cylindrical pile models)	3D (Spherical pile models)
no (uncoupled)	Terzaghi (1923)	Soderberg (1962)	Torstensson (1975)
$v$ - $v$ (coupled 1)	Imre (1997-1999)	Imre & Rózsa (1998)	Imre & Rózsa (2002)
$v$ - $\varepsilon$ (coupled 2)	Biot (1941)	Randolph et al (1979)	Imre & Rózsa (2005)

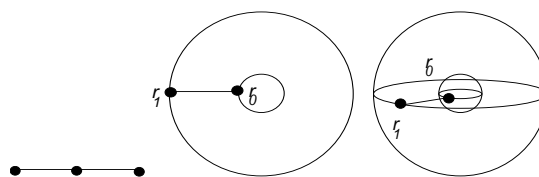


**Fig. 6.** The displacement domain bounded by a (a) 0 dimensional sphere (oedometer model), (b) 1 dimensional sphere (cylindrical model), (c) 2 dimensional sphere (spherical model).

## 7. Example 2 - dissipation test evaluation

The objective of the study was to elaborate automatic evaluation methods for such dissipation tests of Geotechnics that can be evaluated with linear, point-symmetric, coupled consolidation models [9 to 16] (Tables 1 to 3).

The follower merit function related to these injective, analytical consolidation model solutions, with fixed, convex initial condition and sufficiently long data series is strictly convex, according to the experiences [11]. However, by the identification of the initial condition on a function class allowing non-convex analytic functions and by modelling of relaxation (time dependent constitutive law), this geometry may slightly change, but remains near-convex. The same method - applying the global coordinate grid projection algorithm - was applicable in every case (software is available for each case [18 to 23]).

In case of the standard multistage oedometric compression tests (MCT) and its dual counterpart, the multistage oedometric relaxation tests (MRT), a short testing procedure (with shorter stages than 99% of the dissipation time except for the last stage) was suggested. Laboratory tests were made on identical soil samples with different plasticity [9, 10]. The model validation showed that (i) the fitting error decreased to half for those model-variants where the simultaneous creep/relaxation was considered, (ii) the relaxation qualitatively influenced the model response in a parameter dependent way, and (iii) the short stage data were successfully evaluated using the clever section of the single parameter  $c$ .

In this paper a summary is given on the evaluation of the multistage oedometric relaxation tests MRT. It is shown, that by using the suggested technique, a class of inverse problems - being related to (near-)convex follower merit functions - becomes easily soluble without iteration or regularization, the reliability criteria of the solution can be readily be tested.

## 7.1 Model-versions

### 7.1.1 Analytical solution

The analytical solution of the linear, point-symmetric coupled consolidation model of the oedometric relaxation test for the so called total stress  $\sigma$  and the so called pore water pressure  $u$  (Appendix A to C [8 to 11]):

$$\sigma(t) = - \sum_{i=1}^{\infty} \varphi_i e^{-i^2 \pi^2 T} + \sigma_{\infty} \quad (20)$$

$$u(t, y) = - \sum_{i=1}^{\infty} \varphi_i [\cos(y(i \pi / H) - 1)] e^{-i^2 \pi^2 T} \quad (21)$$

where  $T = ct/H^2$  is the time factor,  $c$  is the coefficient of consolidation,  $\varphi_i$  are Fourier coefficients related to the initial condition,  $H$  is the half-width of a double-drained sample (length between the boundaries of the model).

The linear, coupled consolidation model consolidation model has some special features, which can be summarized as follows ([8 to 11]). Being the volume constant during a stage, the mean effective stress ( $\sigma_{mean}$ ) is equal to the final total stress ( $\sigma_{\infty}$ ) which depends on the displacement load  $v_0$  and the  $H$  the sample height:

$$\sigma_{\infty} = \frac{E_{oed} v_0}{H} \equiv \sigma'_{mean}(t) \quad (22)$$

The time dependent constitutive law was included in an approximate form into the model in its most complex form, by adding a relaxation term to the total stress. The relaxation term includes a partial unloading effect. The equations used for model fitting were as follows.

$$\sigma(t) = - \sum_{i=1}^{\infty} \varphi_i e^{-i^2 \pi^2 T} + \sigma_{\infty} - \Delta \sigma^r(t) \quad (23)$$

The empirical relaxation term:

$$\Delta \sigma^r(t) = s \sigma(0) \frac{1}{1 - sb} \log \left( \frac{t + t_1}{t_1 + t_3} \right); t > t_3 \quad (24)$$

where  $s$  is the coefficient of relaxation,  $t_3$  is the pause of relaxation in case of partial unloading,  $b=\log((t_1+t_3)/t_1)$ ,  $t_1$  is time parameter.

### 7.1.2 Model-versions for parameter identification

The initial condition was identified using the following parametric shape function in model H:

$$u(0,y)=A y^3 + B y^2 + C y \quad (25)$$

where  $A$ ,  $B$  and  $C$  are real valued initial condition parameters, with linear dependence. The related Fourier coefficients were included in the model.

The model H contained 8 parameters, 4 out them were with non-linear dependence (Table 4). The linearly dependent  $A$ ,  $B$  and  $C$  parameters equally allowed convex, concave or partly convex and concave initial condition functions. Several model-versions were elaborated, differing in the number of the non-linearly dependent parameters, using additional information on the consolidation part-model and the relaxation part-model (described in Appendix B and C), in here only model-version HC is mentioned where no relaxation was modeled.

It can be noted that parameters  $\sigma_\infty$  and  $c$  have different meaning if relaxation is modelled or if not. If the relaxation is modelled, the compression curve constructed from the identified  $\sigma_\infty$  is time independent, this is the so called instant compression curve. However, if the relaxation is not modelled (ie., for model-version HC), the identified  $\sigma_\infty$  is depending on the stage duration, as it is dependent in the measurements (as it is well-known from the oedometer testing).

## 7.2 Algorithms for parameter identification

### 7.2.1 Conjugate gradients with a new starting vector algorithm

- The model-version H was fitted on measured data with the conjugate gradient method. However, the solution was not possible to be determined due to the large number of critical points. Therefore, a local grid system was used to determine some new starting vectors.
- The grids were 2-dimensional, considering the most important parameters ( $c$ , initial condition).

### 7.2.2. Projection algorithm

- The model-version H and HC were fitted on measured data with the projection algorithm including linear subminimisation [8 to 11], in the frame of an automatic global minimization (Fig. 3).
- The coordinate mesh was generated in the subspace of the non-linearly dependent parameters, since the linearly dependent parameters can be eliminated by subminimisation.
- The grid was defined by using the half error domain diameter values of some preliminary simulations, regarding the clever section of noisy and the follower, noise-free merit functions.
- The one-dimensional clever sections were approximately determined by a projection algorithm, using real-life merit function values in the points of a coordinate grid.
- Once the minimum of the real-life merit function was determined, the same algorithm was reused to determine the one-dimensional clever sections of the follower merit functions, too. The difference them at the global minimum were used to determine the error domain and, to observe uniqueness under the effect of added non-linearities.

## 7.3 Results

### 7.3.1 New starting vector method

Three successive iteration steps, including the conjugate gradient starting and ending points and coarse grids centered the ending critical points determined by the conjugate gradient method are shown in Figure 7. The section along the fold of the projection within the local grids were represented, revealing the complex geometry of the merit function (Fig. 7). The success of the local grid was apparent but no reliability information was found for the solution and the computational work was excessive.

### 7.3.2. Split inverse problem solution (projection algorithm and clever sections)

The projection algorithm was used with linear subminimization according to Fig. 3. In case of model-version H a 4-dimensional coordinate grid was used, the four one-dimensional clever sections were determined by projection and a subsequent minimization for of the real-life and the follower merit functions. In case of model-version HC, 1-dimensional grid was used to determine the clever section of the real-life and the follower merit functions for parameter  $c$ .

The clever section of parameter  $c$  determined for the two model-versions were similar, indicating two minima both models (Fig. 8), one minimum was related to a nice, physically admissible initial condition, another to a physically non-admissible one.

The compression curve points ( $\sigma_\infty$ ) were determined by model HC from each stage. In case of short stages, the good minimum was quasi-degenerated (Fig. 9). Evaluating the short stages with the simplest model HC, the implicit function  $g(c)$  was determined for each stage only. From function  $g(c)$ , by using the  $c$  identified from the last, long stage, the global minimiser vector and parameters  $\sigma_\infty$  were selected. The latter gave compression curve points, being situated above the one determined by the long compression test in accordance with the expectations following from the time dependency of the constitutive law (Fig. 9).

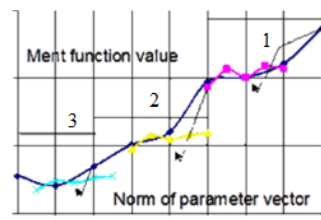


**Fig. 7.** The complexity of the topography, implicit functions at three successive steps, fine and coarse local grids. Conjugate gradient method (with arrows) ([16]).

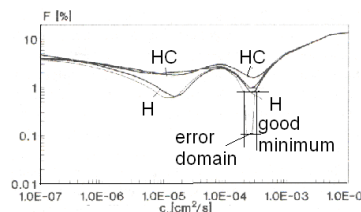


**Fig. 8.** Model H and HC, long stage, clever sections  $c$ . Note the non-unique solution for both models ([14]).

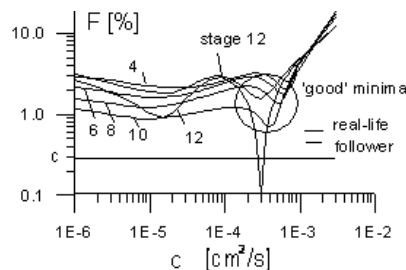
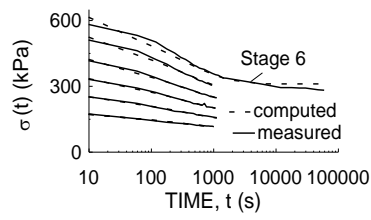
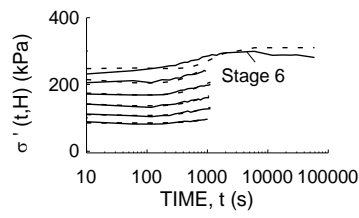


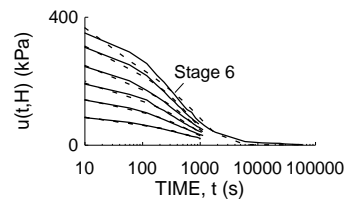
**Fig. 9.** Model HC, short stages 1 to 11 and last, long stage 12. The clever sections  $c$  is quasi-degenerated (stages 1 to 11) and there are two minima for the long stage 12. The  $c$  identified from the last stage was used for the evaluation of the short stages ([14]).



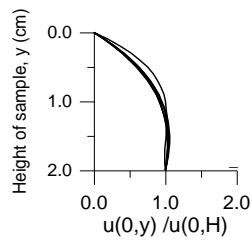
(a) Total stress.



(c) Effective stress.



(b) Pore water pressure.



(d) Identified initial condition in the various stage.

**Fig.10.** MRT, fitted and measured stresses

**Table 4.** Parameters of the most general oedometric model-version H

Model	Parameter	Symbol	Dependence
Consolidation	Initial condition	A, B, C	linear
	Coeff. of consolidation	$c$	nonlinear
	asymptotic total stress	$\sigma_{\infty}$	linear
Relaxation	coefficient of relaxation	$s$	nonlinear
	pause of relaxation	$t_3$	nonlinear
	delay time	$t_l$	nonlinear

**Table 5.** Parameters of the consolidation oedometric relaxation test model-version HC

Model	Parameter	Symbol	Dependence
Consolidation	initial condition	A, B, C	linear
	Coeff. of consolidation	$c$	nonlinear
	asymptotic total stress	$\sigma_{\infty}$	linear

Table 6. Grid sizes of oedometric relaxation test, model-version HC

Model-version	H	HC
Parameter # (linear)	4	4
Parameter # (non-linear)	4	1
# of global mesh points	125000	54

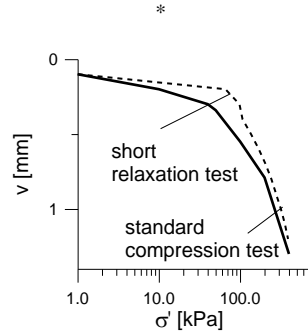


**Fig. 11.** Compression curves -constructed from final total stress parameters, identified from various stages, using Model HC. The  $c$  identified from the last stage was used for the evaluation of the short stages.

## 8. Discussion, conclusion

### 8.1 The hierarchical minimisation

Geometrically, let us determine the fold of such a map which is the orthogonal projection of the graph of the merit function onto a coordinate plane  $\langle F, \mathbf{x} \rangle$ , where  $\mathbf{p}=(\mathbf{x}, \mathbf{y})$  is a direct sum decomposition of the parameter space and the Hessian with respect to  $\mathbf{y}$  is globally positive definite. The implicit function  $\mathbf{g}(\mathbf{x})$  of the derivative of the projection with respect to  $\mathbf{y}$  can be determined by sub-minimization at every fixed  $\mathbf{x}$ . Therefore, the non-linear minimisation of an analytic merit function can be split in terms of dimension. In the first part of the split inverse problem the section along the graph of the implicit function (i.e. along the fold)  $F[\mathbf{g}(\mathbf{x}), \mathbf{x}]$  - called clever section - is determined subminimisation, then the clever section is minimised. Two different minimisation methods can be used at two parts of the direct sum decomposition of the parameter domain.

The most important practical application in minimisation is the elimination of the linear part of parameter vector through sub-minimization, which can be added to any algorithm. The linearly dependent parameters can be eliminated by sub-minimization before each function value evaluation.

Another important practical application could be the case of the quasi-degenerate minimum. The  $\mathbf{g}(\mathbf{x})$  can be used to estimate the global minimum of  $F[\mathbf{x}, \mathbf{g}(\mathbf{x})]$  without minimization it, on condition that independent knowledge is available for  $\mathbf{x}_{\min}$ . By using the known parameter vector value  $\mathbf{x}_{\min}$  of the global minimum, since  $\mathbf{y}_{\min} = \mathbf{g}(\mathbf{x}_{\min})$ . This follows from the fact that the implicit function is analytic, simple curve.

The one-dimensional clever section  $F[\mathbf{g}(x_i), x_i]$  of the merit function related a parameter  $x_i$  can be used to determine the diameter of the error domain with respect to  $x_i$  and to test uniqueness. For those model-versions where the clever section is at least two-dimensional with the form  $F[\mathbf{x}, \mathbf{g}(\mathbf{x})]$  and, the follower merit function is convex, the one-dimensional clever sections can approximately be determined by a projection algorithm suggested here.

The follower merit function is not known a priori but can be constructed once Hierarchical global minimiser is known. In this way it can be used in reliability testing, can be used to define a parameter error domain and to define uniqueness criteria.

### 8.2 Follower merit function

The concept of the follower, noise-free merit function (i.e. the best, noise-free approximation of the real-life merit function) was introduced, which is close to the real-life merit function except in the vicinity of the global minimiser.

The difference between the follower and the real-life merit function is bounded by a term in Eq (12) which is controlled by the noise-free merit function, which is a pseudo-metric, expressing the distance of a given parameter vector from the global minimum, where its value is zero.

The follower merit function can be used in minimisation to skip the local minima on the similarity domain. The decreasing direction can be found if the step size is large enough. This can be realized by adjustable step size (e.g. being dependent on the actual fitting error) or fixed step size (~ eg., related to the diameter of the error domain). Further research is needed on this.

Concerning convexity, the following comment can be made. There is a false opinion that no bracketing procedure can be used in multidimensional space since The merit function is always with complex geometry [1]. However, there is an ideal exception which is the class of the is strictly convex minimisation. Hyperplanes generated by coordinate a mesh points can bracket decreasing convex level surfaces in multidimensional case.

In case of real-life inverse problems, only the follower, noise-free merit function can be strictly convex due to the noise and, the convexity can be used on the similarity domain. According to the experiences, this may be the case in case of the injective solutions of linear system of PDE-s, in case of fixed, convex initial condition and sufficiently long data series. By the identification of the initial condition and by modelling of relaxation (time dependent constitutive law), this geometry slightly changed (see example 2).

### 8.3 Conclusions

The results of the study can be concluded as follows.

- 1) The multi-dimensional implicit function theorem can be applied for the  $y$ -derivative of a projection map related the graph of a merit function onto a vertical coordinate plane, generated by the complement  $\mathbf{x}$ , where  $\mathbf{p}=(\mathbf{x},\mathbf{y})$  is a direct sum decomposition of the parameter space. The implicit functions in case of strictly convex merit function are globally unique and have the same lattice structure as the subspaces of the direct sum decomposition.
- 2) The real-life merit functions have an unimaginable complexity of an  $M$ -dimensional topography, where  $M$  is the number of the parameters. However, there is an underlying noise-free merit function, called follower merit function which can be constructed from simulated, noise-free data using the solution of a Least Squares minimization. The relatively small difference between the follower, noise-free and the real-life, noisy merit functions is controlled by the value of the follower noise-free merit function, which is a pseudo-metric, (expressing the distance from the global minimum, where its value is zero).
- 3) In the case of strictly convex, noise-free functions, the bracketing of the level surfaces is theoretically possible on the  $M$ -dimensional topography by the hyperplanes of a properly selected coordinate grid (generated in the parameter space). This can approximately be done for follower merit functions, using real-life merit function values on the similarity domain.

The consequences in minimisation and parameter identification as follows.

- The implicit function  $\mathbf{g}(\mathbf{x})$  of the derivative of the projection with respect to  $\mathbf{y}$  can be determined by sub-minimization at every fixed  $\mathbf{x}$  and, and the so called section along the graph of the implicit function  $F[\mathbf{g}(\mathbf{x}), \mathbf{x}]$  is minimised by unconditional minimisation. Therefore, two different minimisation methods can be used at two parts of the direct sum decomposition of the parameter domain related to the projection.
- The most important practical application in minimisation is the elimination of the linear part of parameter vector through sub-minimisation, which can be added to any algorithm. The linearly dependent parameters can be eliminated by sub-minimisation before each function value evaluation.
- Another important practical application could be the case of the quasi-degenerate minimum. The injective  $\mathbf{g}(\mathbf{x})$  can be used to estimate the global minimum of  $F[\mathbf{x},\mathbf{g}(\mathbf{x})]$  without minimization it, on condition that independent knowledge is available for  $\mathbf{x}_{\min}$ . By using the known parameter vector value  $\mathbf{x}_{\min}$  of the global minimum, since  $\mathbf{y}_{\min} = \mathbf{g}(\mathbf{x}_{\min})$ .
- Another practical application is related to the case of the use of the one-dimensional clever section  $F[\mathbf{g}(x_i), x_i]$  of the merit function. This is a kind of deepest section with respect to the specified parameter  $x_i$ . It can be used to determine the diameter of the parameter error domain and to define uniqueness criteria.

- Combining the basic results, in case of strictly convex follower merit functions, the one-dimensional clever sections related to the individual parameters can approximately be determined by the suggested projection algorithm (based on nested cycle coordinate grid computations of the real-life merit function, with minimum search). These sections can be used in minimization and reliability testing, being the deepest possible sections with respect to a given parameter. For those model-versions where the clever section is at least two-dimensional with the form  $F[x, g(x)]$  and, the follower merit function is convex, the one-dimensional clever sections can approximately be determined by a projection algorithm suggested here.

Some practical consequences can be mentioned as follows.

- In the secant method, the step size depends on the merit function value. Therefore, the step size is comparable to the size of the irregularities of the real-life merit function with respect to the follower merit function on the similarity domain. Therefore, the secant – type non-linear parameter identification methods can theoretically be useful for most parameter identification problems.
- Some non-iterative, non-linear parameter identification methods were elaborated related to linear, coupled point-symmetric consolidation models (Table 3) by using the suggested global coordinate grid method and clever section information in case of quasi-degenerated minima (software is available).

Further research is suggested, among others

- on the convexity of the follower merit functions related to injective solutions of system of coupled, linear partial differential equations; including the effect of non-convex initial conditions and an added non-linearity;
- on the difference between real-life and convex follower merit functions, by using one-dimensional clever sections;
- on the differences between the various (statistical and geometrical) parameter error domains in the light of the true error sizes;
- on the step size of the multidimensional minimization methods which do not use one-dimensional minimization, the adjustment to skip the local minima;
- on the application of the hierarchical minimisation for the systems of non-linear equations.

## References

- [1] Press, W.H.; Flannery, B.P.; Teukolski, S.A.; Vetterling, W.T. (1986): Numerical Recipes. Cambridge Univ. Press.
- [2] Meier J, Rudolph, S., Schanz T: Effective Algorithm for parameter back calculation - Geotechnical Applications published in: Bautechnik Volume 86 Issue S1, 86 - 97
- [3] Hegedus, Cs (2008): Numerikus Analízis, egy. jegyzet, ELTE, IK, <http://www.inf.elte.hu/karunkrol/digitkonyv/Jegyzetek2008/numanal.pdf>, Budapest.
- [4] Milnor, J.W. (1963) Morse theory. Princeton University Press. 153 p.
- [5] Szökefalvi-Nagy, Gy; Gehér, L.; Nagy, P. (1979) Differential geometry. Műszaki Könyvkiadó, Budapest. 256 p.
- [6] Wolfe, P. (1959). The secant method for simultaneous nonlinear equations. *Comm. of ACM*, 2, pp. 12-13.
- [7] Berzi P, Imre E (1998) Parameter identification by the amended secant method. In: Delaunay, D; Jarny, Y; Woodbury, K A (szerk.) Proceedings of the 2nd International Conference on Inverse Problems in Engineering Fairfield (NJ), USA: American Society of Mechanical Engineers (ASME), (1998) ..
- [8] Berzi P (2021) Root-finding of a nonlinear function with an updated secant method. *Int. Conf. on opt. and Appl.* submitted.
- [9] Imre, E., Vijay P. Singh and Fityus S. (2013). The modelling of some point-symmetric tests 166-185. *Proc. of the 3rd Kézdi Conference. Budapest, Hungary*, 2013.05.28. ISBN 978-963-313-081-0.
- [10] Imre, E. (1995). Model discrimination for the oedometric relaxation test. *Proc. of 8-th Baltic Geotechnical Conference*, 55-60.
- [11] Imre, E. (1995). Model discrimination for conventional step-loaded oedometric test. *Proc. of the Int. Symp. on Compression and Cons. of Clayey Soils, IS-Hiroshima'95*, 525-530.
- [12] Imre, E.; Rózsa, P.; Bates, L.; Fityus, S (2010) Evaluation of monotonic and nonmonotonic dissipation test results. *Computers and Geotechnics*, 37, Issues 7-8, 885-904. DOI: 10.1016/j.compgeo.2010.07.008
- [13] Imre E, Schanz T, Hegedüs Cs (2013) Some thoughts in non-linear inverse problem solution. *EURO:TUN* .
- [14] Imre, E (1998) Inverse problem solution with a geometrical method 1998 In: Delaunay, D; Jarny, Y; Woodbury, K A (szerk.) Proceedings of the 2nd International Conference on Inverse Problems in Engineering Fairfield (NJ), USA: American Society of Mechanical Engineers (ASME), (1998) pp. 331-338. , 8 p.
- [15] Imre, E; Hegedüs Cs; Kovács S. (2018) Some Comments on the Non-Linear Model Fitting IEEE 18th International Symposium on Computational Intelligence and Informatics (CINTI 018) Budapest, Hungary

- [16] Imre, E. Trang, Q.P Fityus, I. Telekes, G (2011) A geometric parameter error estimation method. ComGeo II.405-414.
- [17] Advanced General Purpose Inverse Problem Evaluation Software EVA
- [18] Advanced Engineering Evaluation Software CPTu dissipation test, Imre-Rózsa model 2D
- [19] Advanced Engineering Evaluation Software CPTu dissipation test, Randolph-Wroth model 2D
- [20] Advanced Engineering Evaluation Software CPTu dissipation test, Imre-Rózsa model 3D
- [21] Advanced Engineering Evaluation Software Compression test (MCT), (modified) Bjerrum model (AC, BC) models
- [22] Advanced Engineering Evaluation Software Compression test (MCT), (modified) Terzaghi model(A,B) models
- [23] Advanced Engineering Evaluation Software Oedometric relaxation test (MRT), Imre-models (H, HC, HCR, HCRT)

Appendix

Example for the introduced definitions at Least Squares inverse problem

Let us assume the following model with a linearly dependent parameter  $a$ :

$$u(t, x) = at^2x \quad (26)$$

where  $t$  is the time variable  $x$  is the space variable,  $a$  is the parameter.

Simulated data vector assuming  $x = 1, t = [1, 2, 3]$ ,  $a = 2$  (i.e. fixed values for the sampling times, the space variable and parameter  $a$ ):

$$f' = \begin{bmatrix} 2 \\ 8 \\ 18 \end{bmatrix} \quad (27)$$

Noisy data vector and noise vector:

$$f_m = \begin{bmatrix} 2.1 \\ 7.8 \\ 18.2 \end{bmatrix}, \quad (28)$$

$$z = \begin{bmatrix} 0.1 \\ -0.2 \\ 0.2 \end{bmatrix},$$

System of equations (noisy problem):

$$Aa = f_m \quad (29)$$

System of equations (noise-free problem):

$$Aa = f \quad (30)$$

where matrix  $A$  is as follows (the derivative of the model with respect to  $a$  at fixed value of the sampling time vector and the space variable):

$$A = \begin{bmatrix} 1 \\ 4 \\ 9 \end{bmatrix} \quad (31)$$

In detail, the system of Equations for the noise-free problem:

$$\begin{bmatrix} 1 \\ 4 \\ 9 \end{bmatrix} a = \begin{bmatrix} 2 \\ 8 \\ 18 \end{bmatrix} \quad (32)$$

In detail, the system of Equations for the noisy problem

$$\begin{bmatrix} 1 \\ 4 \\ 9 \end{bmatrix} a = \begin{bmatrix} 2.1 \\ 7.8 \\ 18.2 \end{bmatrix} \quad (33)$$

The solution can be determined by the Gauss Normal Equations:

$$A^T A a' = A^T f_m \quad (34)$$

Solution with the Gauss Normal Equations for the noise-free problem:

$$A^T A a = A^T f \quad (35)$$

In detail:

$$A^T A = 98 \quad A^T f = 196 \quad a = 2 \quad (36)$$

Solution with the Gauss Normal Equation for the noisy problem:

$$A^T A = 98 \quad A^T f_m = 197.1, \quad a' = 2.011224 \quad (37)$$

Simulated data vector assuming  $x = 1, t = [1, 2, 3]$ ,  $a = 2.011224$  (i.e. fixed values for the sampling times, the space variable and parameter  $a$ ):

$$f' = \begin{bmatrix} 2.011224 \\ 8.044896 \\ 18.101016 \end{bmatrix} \quad (38)$$

Real-life merit function:

$$F(a) = (2.1 - a)^2 + (7.8 - 4a)^2 + (18.2 - 9a)^2 \quad (39)$$

The simulated, noise-free merit function related to then true value of the parameter  $a$ :

$$F'(a) = (2 - a)^2 + (8 - 4a)^2 + (18 - 9a)^2 \quad (40)$$

The follower, simulated noise-free merit function, related to the solution of the noisy inverse problem, the identified value of parameter  $a$ :

$$F''(a) = (2.011224 - a)^2 + (8.044896 - 4a)^2 + (18.101016 - 9a)^2 \quad (41)$$

The clever sections of the noisy and the follower merit function for parameter  $a$  are shown in Fig. 2. The true error ( $\sim 0.011$ ) is equal to about 1/5 of the width of the error domain ( $\sim 0.056$ ) or about 4/10 of the half width of the error domain called generalized standard deviation.

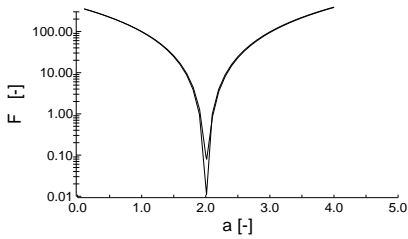


Fig. 12. The clever sections of the noisy and the follower merit function for parameter  $a$

## Appendix A The consolidation model

The point-symmetric, linear coupled consolidation models can be summarized into a single mathematical model in the function of the embedding space dimension  $m$  (Fig 1, oedometric  $m=1$ , cylindrical  $m=2$ , and spherical models  $m=3$ ). For every embedding space there are two models differing in one boundary condition. In this section the linear coupled consolidation models elaborated for the relaxation/compression test models ( $m=1$ ) are presented.

### 1) System of differential equations

Two equations have been derived from the equilibrium condition and, from the continuity condition, assuming weightless soil and water. The Equilibrium Equation compiles the equilibrium condition, the effective stress equality, the geometrical and, the constitutive equations, as follows:

$$E_{oed} \frac{\partial \varepsilon}{\partial y} - \frac{\partial u}{\partial y} = 0 \quad (42)$$

and, the Continuity Equation compiles the continuity equation, the Darcys law and the geometrical equation, as follows:

$$-\frac{k}{\gamma_v} \Delta u + \frac{\partial \varepsilon}{\partial t} = 0 \quad (43)$$

where  $v$  is displacement,  $u$  is pore water pressure (neglecting the gravitational component of the hydraulic head),  $y$  and  $t$  are space and time co-ordinates respectively,  $E_{oed}$  is the oedometric modulus. The volumetric strain and the Laplacian operator, for dimension  $m=1$  are as follows:

$$\varepsilon = \frac{\partial v}{\partial y}, \Delta = \frac{\partial}{\partial y^2} \quad (44)$$

## 2) Boundary conditions

The displacement domain of the oedometric test is bounded by two zero dimensional circles, with radii  $r=0$  and  $r=H$ , \*respectively. For a double-drained sample, the upper-lower surface coincides with the outer boundary, respectively, the symmetry point coincides with the inner boundary. In the following four boundary conditions are presented. Three are common, one is different for the two models.

(1) The (common) boundary condition Nr. 1:

$$u(t, r)|_{y=0} = 0 \quad (45)$$

(2) The (common) boundary condition Nr. 2:

$$\frac{\partial u(t, y)}{\partial y} \Big|_{y=H} = 0 \quad (46)$$

(3) The (common) boundary condition Nr. 3:

$$v(t, y)|_{y=H} = 0 \quad (47)$$

(4) Boundary condition Nr. 4 concerning the coupled 1 models:

$$v(t, y)|_{y=0} = v_0 > 0 \quad (48)$$

(5) Boundary condition Nr. 5 concerning the compression test models:

$$\varepsilon(t, r)|_{y=0} = \varepsilon_0 > 0. \quad (49)$$

## 3) Analytical solution

Steady-state solution part

The solution for the relaxation test model:

$$v^p(y) = v_0 \left( 1 - \frac{y}{H} \right) \quad (50)$$

$$\sigma^p(y) = -\frac{E_{oed} v_0}{H} \quad (51)$$

and, for the compression test model:

$$v^p(y) = \frac{\sigma_0}{E_{oed}} (H - y). \quad (52)$$

$$\sigma^p(y) = \sigma_0 \quad (53)$$

Transient solution part

The displacement  $v^t$  for the oedometric relaxation test model:

$$v^t(t, y) = \sum_{k=1}^{\infty} a_k \cdot \sin\left(\frac{k \cdot \pi}{H} y\right) \cdot e^{-\frac{k^2 \cdot \pi^2}{H^2} c_v t} \quad (54)$$

where  $a_k$  ( $k=1 \dots \infty$ ) are the Fourier coefficients of an odd initial displacement function and, for the compression test model:

$$v^t(t, y) = \sum_{k=1}^{\infty} b_k \cdot \cos\left(\frac{(2k-1) \cdot \pi}{2H} y\right) \cdot e^{-\frac{(2k-1)^2 \cdot \pi^2}{4H^2} c_v t} \quad (55)$$

where  $b_k$  ( $k=1 \dots \infty$ ) are the Fourier coefficients of an even initial displacement function. The function  $u$  for the relaxation test model:

$$u(t, y) = \sum_{k=1}^{\infty} \alpha_k \left\{ \left[ \cos\left(\frac{k \cdot \pi}{H} y\right) \right] - 1 \right\} e^{-\frac{k^2 \cdot \pi^2}{H^2} c_v t} \quad (56)$$

and, for the compression test model:

$$u(t, y) = \sum_{k=1}^{\infty} \beta_k \sin\left[\frac{(2k-1)\pi}{2H} y\right] e^{-\frac{(2k-1)^2 \cdot \pi^2}{4H^2} c_v t} \quad (57)$$

where

$$\alpha_k = a_k \frac{k\pi}{H}; \beta_k = -b_k \frac{(2k-1)\pi}{2H}; \alpha_0 = -\sum_{k=1}^{\infty} \alpha_k \quad (58)$$

The following two dimensionless arguments  $R$  and  $T$  can be derived for the compression and for the relaxation test model, respectively:

$$Y = \frac{y}{H} \text{ or } Y = \frac{y}{2H} \quad (59)$$

$$T = \frac{ct}{H^2} \text{ or } T = \frac{ct}{4H^2} \quad (60)$$

It follows from the difference of the time factors that the model law is different for the two tests. It also follows that slower dissipation time can be expected for the OCT than for the ORT in case of identical initial conditions.

## Appendix B Qualitative behaviour of the consolidation model

### Stress state in the sample

For the ORT model, the stress variation within the sample is partly rebound, partly compression as follows. The total stress  $\sigma$  is equal to the sum of a steady-state and a transient component. The former - the final total stress  $\sigma_{\infty}$  - depends on the displacement load  $v_0$  and the  $H$  the sample height:

$$\sigma_{\infty} = \frac{E_{oed} v_0}{H} \quad (61)$$

The latter is equal to the mean pore water pressure  $u_{mean}$ :

$$\sigma^t(t) = u_{mean}(t) = \frac{1}{H} \int_0^H u(t, y) dy \quad (62)$$

Effective stress decrease takes place at the sample top ( $y=0$ ), and compression (increase in the effective stress  $\sigma$ ) takes place in the bottom ( $H=0$ ) of the sample

$$\varepsilon^t(t, y) = -\frac{1}{E_{oed}} [u_{mean}(t) - u(t, y)] \quad (63)$$

For the OCT model, the total normal stress is constant with time. The effective normal stress increases with time, since its transient part is equal to the pore water pressure and the consolidation model predicts basically the compression.

$$\varepsilon^I(t, y) = \frac{1}{E_{oed}} u(t, y) \quad (64)$$

#### Appendix C Simplification of joined model parameters

The analytical solution of model-version *H* contains 8 parameters, 4 out them are with non-linear dependence (Table 1). In model-version HCRT parameter *t1* was specified, *b* was zero and, a minor change was made in the way of the identification of the relaxation parameter *s* as follows. The product of *s* and  $\sigma(0)$  denoted by *sk*

$$sk = s \sigma(0) \quad (65)$$

was identified instead of *s*. The solution depends linearly on *sk*. As a result, the number of the non-linearly dependent parameters was decreased to 2 and, the computational work was less by two orders of magnitude than the one for model *H*.

In model-version HCR value of *t3*, *t1* were specified, the modified relaxation parameter (*sk*) was identified instead of *s* using the facts that term  $\sigma(0)$  can be expressed as the linear combination of other parameters:

$$\sigma(0) = \sigma_{\infty} + D \quad (66)$$

where *D* is the mean initial pore water pressure. In model-version HCR only one among the three parameters of the relaxation part-model was identified (*sk*), value of *t3* was set to zero. The relaxation branch of the model was left out in model-version HC (Table 2). The number of the non-linearly dependent parameters was 1 and, the computational work was less for these than for any other model-versions (Table 3).

